Liquid Crystals
Publication details, including instructions for authors and subscription information:
http://www.informaworld.com/smpp/title~content=t713926090

X-ray diffraction study on liquid crystals from 4-hexylphenyl 4-cyanobenzoyloxybenzoate and 4-heptyloxyphenyl 4-cyanobenzoyloxybenzoate

Z. X. Fan[a]; L. Y. Chiang[b]; W. Haase[a]
[a] Institut für Physikalische Chemie, Technische Hochschule Darmstadt, Darmstadt, Germany [b] Corporate Research Science Laboratory, Exxon Research and Engineering Company Annandale, New Jersey, U.S.A.

To cite this Article Fan, Z. X. , Chiang, L. Y. and Haase, W.(1995) 'X-ray diffraction study on liquid crystals from 4-hexylphenyl 4-cyanobenzoyloxybenzoate and 4-heptyloxyphenyl 4-cyanobenzoyloxybenzoate', Liquid Crystals, 18: 1, 13 — 19
To link to this Article: DOI: 10.1080/02678299508036585
URL: http://dx.doi.org/10.1080/02678299508036585

LIQUID CRYSTALS, 1995, VOL. 18, NO. 1, 13–19

X-ray diffraction study on liquid crystals from 4-hexylphenyl 4-cyanobenzoyloxybenzoate and 4-heptyloxyphenyl 4-cyanobenzoyloxybenzoate

by Z. X. FAN†, L. Y. CHIANG‡ and W. HAASE*†

† Institut für Physikalische Chemie, Technische Hochschule Darmstadt, Petersenstrasse 20, 64287 Darmstadt, Germany

‡ Corporate Research Science Laboratory, Exxon Research and Engineering Company Annandale, New Jersey 08801, U.S.A.

(*Received 22 October 1992; in final form 31 March 1994; accepted 19 April 1994*)

X-ray investigations were performed on 4-hexylphenyl 4-cyanobenzoyloxybenzoate (DB6CN) and on 4-heptyloxyphenyl 4-cyanobenzoyloxybenzoate (DB7OCN). For both compounds, the smectic A_2 structure is observed. From the small angle meridional reflections, the angular distribution of the smectic units around the normal to the smectic layers and the longitudinal correlation length were studied. The orientational order parameter is calculated from the wide angle equatorial reflections. Based on the assumption of a layer structure with undulation in the liquid crystalline smectic A phase, the relationship between the dimensionless parameters χ_{coh}/d_L (correlation length/thickness of the smectic layer) and FWHM/$2\theta_0$ (full width at the half maximum/maximum point of the scattering peak) is simulated.

1. Introduction

The low ordered liquid crystalline smectic phases consist microscopically of many small distorted regions with finite size, the so-called microdomains [1]. Within the microdomains, the smectic layer structure is deformed because of the liquid behaviour of the molecules within the layers and the weak interaction between the layers. Fortunately, the X-ray diffraction technique provides an excellent tool to investigate deformed liquid crystal structures and the ordering within the smectic layers.

Recently, a scattering model for the stacking structure of smectic layers with undulation was described [2, 3]. In the present paper, assuming the validity of this model, the relationship between ξ_{coh}/d_L (correlation length/thickness of the smectic layer) and FWHM/$2\theta_0$ (full width at the half maximum/maximum point of the scattering peak) will be simulated. Besides this, an attempt to calculate the angular distribution of the smectic microdomains from the small angle meridional reflections is made. Experimentally, the X-ray diffraction studies were performed on two thermotropic liquid crystalline compounds, namely 4-hexylphenyl 4-cyanobenzoyloxybenzoate (DB6CN) and 4-heptyloxyphenyl (4-cyanobenzoyloxybenzoate (DB7OCN). The correlation length, the angular distribution of the smectic microdomains and the orientational order parameters are investigated.

* Author for correspondence.

2. Theoretical background

2.1. *The structural deformation and correlation length ξ_{coh} in the smectic A phase*

A typical deformation of the smectic A structure is undulation of the smectic layers, as shown in figure 1 (*a*), which is due to the weak interaction between neighbouring layers. For every primary point, the secondary scattering points in neighbouring layers are distributed around the normal to the smectic layers [2, 3]. In consequence, the structure factor F can be extracted approximately by integration along a curved secondary scattering front.

An extreme case in this context is the intra-layer scattering in the low ordered liquid crystalline phases: Resulting from the liquid behaviour of the molecules within the layers, the structure factor can be derived by integration along a complete circular front, i.e. in the form of the Bessel function of the zeroth order J_0.

To describe the structural stability in liquid crystalline phases two other physical quantities should be introduced: The Debye–Waller-factor $\langle u \rangle$ and the correlation length ξ_d. The first defines the structural fluctuation, which is to some extent equivalent to the packing fraction or to the disorder of the molecular shift along the molecular long axis. The second is synonymous with the average size of the microdomains.

Theoretically one can simulate the diffraction picture from the Debye–Waller-factor $\langle u \rangle$, the correlation length ξ_d and the structure factor F. The correlation function $G(r)$,

0267–8292/95 $10·00

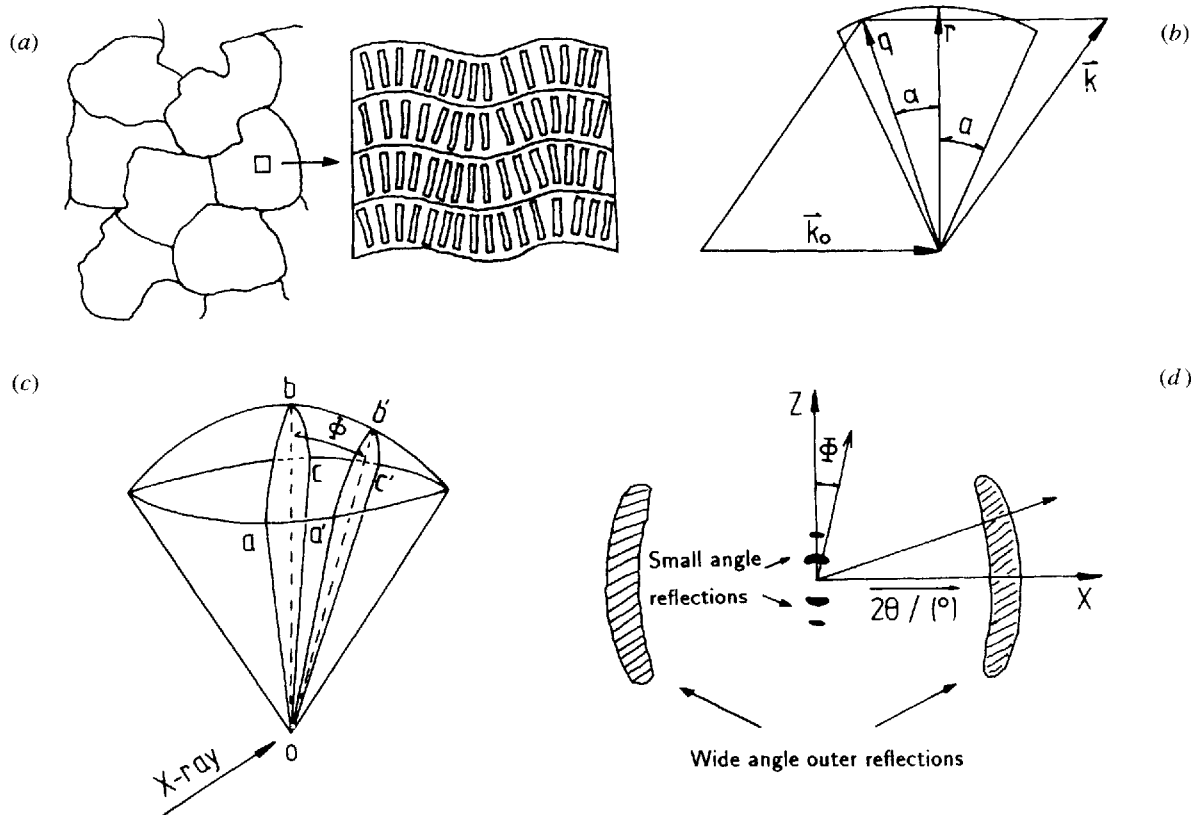

Figure 1. (*a*) Schematic representation of the layer undulation within the liquid crystalline microdomains. (*b*) Vector diagram of the two-dimensional model. (*c*) Three-dimensional representation of the extracted secondary scattering front with an angle Φ between the plane [oabco] and the plane [oa'b'c'o]. (*d*) The scattering pattern in reciprocal space corresponding to the plane [oabco] and the plane [oa'b'c'o] in (*c*).

which can be achieved after Fourier transform of the diffraction data, describes the probability of finding a similar structure. The typical behaviour of $G(r)$ can be characterized in a cosine function, but with a decreased amplitude, apart from the original point. The correlation length ξ_d can be obtained from $G(r)$, until its amplitude converges to $1/e$. In figure 2, the procedures for progressing from the experimental data to the correlation length are schematically represented.

2.2. *The correlation between ξ_{coh}/d_L and the FWHM/2θ_0*

The X-ray diffraction pattern from rod-like molecules in the oriented smectic A phase shows typically a diffuse halo in the wide angle region along the equator, together with one or several sharp reflections in the small angle region along the meridian (see figure 1 (*d*)). The equatorial wide angle diffractions enable us to determine the intermolecular distance for the parallel oriented molecules and the molecular orientation. The meridional small angle reflections belong to the diffraction of the smectic layers. They give us information about the longitudinal correlation length of microdomains and the molecular packing within the layers.

Due to the liquid behaviour at the molecular level within the smectic layers and the large scattering distances given by the small angle meridional reflection, an exact description of the atomic scattering factor is not necessary. According to the undulation scattering model, the elastic scattering amplitude $A(q)$ is defined as

$$A(q) = \int_0^\infty \sigma(r)F(qr, \alpha)\, r\, dr, \tag{1}$$

where σ is the so-called scattering potential [4], α is the distribution angle of the secondary scattering points along the normal of the smectic layers, q is the scattering vector with amplitude $4\pi \sin\theta/\lambda$, and r is the scattering distance. In the smectic A phase, the structure factor F can be defined as [2]

$$F(qr, \alpha) = \int_{-\alpha_{max}}^{+\alpha_{max}} \exp(iqr\cos\alpha)d\alpha \tag{2}$$

$$= \int_{-\alpha_{max}}^{+\alpha_{max}} [\cos(qr\cos\alpha) + i\sin(qr\cos\alpha)]\, d\alpha, \tag{3}$$

where α_{max} is the angular distribution limitation of the structure factor, i.e. the maximal tilt angle of the smectic

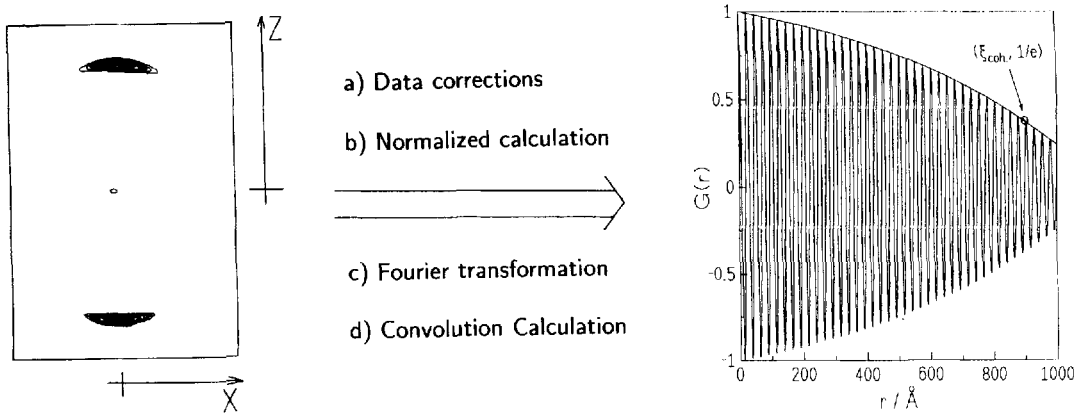

Figure 2. Evaluating process to obtain the longitudinal correlation length from the small angle inner reflection.

layers around the normal of the smectic layers. Since equation (3) can be expanded in a series of Bessel functions, the correlation function can be acquired after the Hankel transformation of the scattering amplitude $A(q)$ and the convolution calculation on the scattering potential $\sigma(r)$:

$$G(r) = H^{-1}[A(q)A^*(q)] = \sigma(r)^*\sigma(-r)$$
$$= \int_{-\infty}^{\infty} \sigma(u)^*\sigma(u+r)\,du \tag{4}$$
$$= \int_{-\infty}^{+\infty} \left\{ \int_0^{\infty} \sqrt{[I(q)]}F(qu,\alpha)q\,dq \times \int_0^{\infty} \sqrt{[I(q)]}F[q(u+r),\alpha]q\,dq \right\} du. \tag{5}$$

where $I(q)$ is the normalized diffraction profile related to the normal to the smectic layers. The evaluation process in going from the diffraction data to the normalized diffraction data is described in [3]. The Hankel transformation can be understood as the Fourier transformation in a two-dimensional space.

Normally, the diffraction curve in the liquid crystalline smectic A phase can be fitted satisfactorily using the Lorentz-function [6]

$$I(\theta) = I_{\max}\left[1 + A\frac{(2\theta - 2\theta_0)^2}{\mathrm{FWHM}^2}\right]^{-2}, \tag{6}$$

where the constant A amounts to $4(\sqrt{2}-1)$. The scattering angle θ is defined as

$$\theta(q) = \arcsin(q\lambda/4\pi). \tag{7}$$

As described in our former paper [3], the angular limitation $\alpha_{\max}$ in equations (2) and (3) was empirically derived from the average values of $\langle\mathrm{FWHM}\rangle$ and $\langle 2\theta_0\rangle$ (see figure 3)

$$\alpha_{\max} = \arccos\frac{\sin(\langle 2\theta_0(\Phi)\rangle - \langle \mathrm{FWHM}(\Phi)\rangle)}{\sin(\langle 2\theta_0(\Phi)\rangle + \langle \mathrm{FWHM}(\Phi)\rangle)}. \tag{8}$$

As shown in figure 2, the correlation length ξ_{coh} can be extracted from the correlation function $G(r)$, until its amplitude converges to $1/e$ [7]. It was found that the relation between ξ_{coh}/d_L and $\mathrm{FWHM}/2\theta_0$ is nearly independent of $2\theta_0$ for relatively large distances. In figure 4, ξ_{coh}/d_L is plotted versus $\mathrm{FWHM}/2\theta_0$. The relation can be described approximately using

$$\ln\frac{\xi_{coh}}{d_L} = -1{\cdot}8885266 - 0{\cdot}9924302\ln\frac{\mathrm{FWHM}}{2\theta_0}. \tag{9}$$

For a finite crystalline system, similarly to the multiplying slits system [8], the correlation length ξ_{coh} can be directly derived from the reciprocal peak profile using $\xi_{coh} = \lambda/\Delta 2\theta$ [9]. On the assumption of perfect alignment of the smectic layers, which only allows a one-dimensional fluctuation along the normal to the smectic layers, many modified theories for the calculation of the correlation length in quasi-long-range smectic phases exist [10, 11]. The remarkable difference between those direct methods and our undulation curved scattering model lies in the introduction of the angular continuous distribution of the structure factor and its influence on the structural stability.

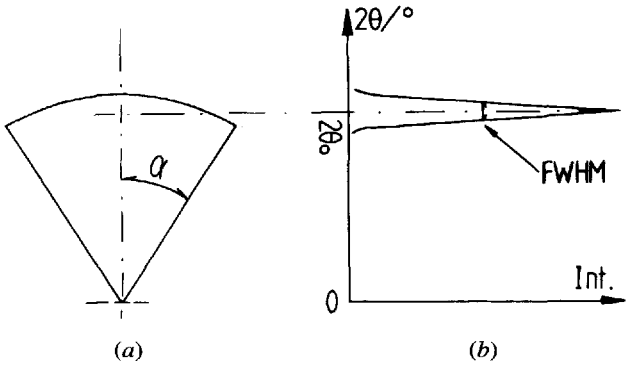

Figure 3. Relationship between the tilt angle α and the scattering profile.

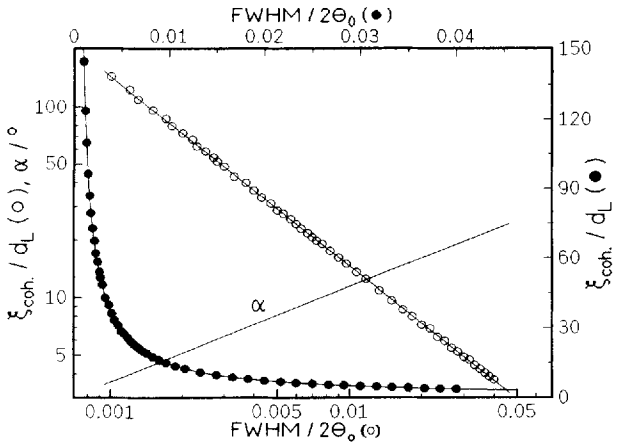

Figure 4. The relationship between ξ_{coh}/d_L and FWHM/$2\theta_0$, represented on linear and logarithmic scales; the profile of angle α versus FWHM/$2\theta_0$ also refers to the logarithmic scale.

Recently, a program was written for simulating the diffraction pictures of smectic A and smectic C phases on the basis of the undulation scattering model. The experimentally observed diffraction patterns in smectic A and smectic C phases agree very well with the calculated data. We will discuss this in a later paper [12].

2.3. *The angular distribution of the smectic layers*

Let us go back to the smectic undulating layer model. Here one can find the diffraction along the direction $\Phi = 0°$ (*Z*-direction in figure 1 (*d*)) which entails the scattering of the smectic layers whose vector traces are geometrically distributed in the [oabco] plane (see figure 1 (*c*)). The diffraction deviating from the *Z*-direction with an angle Φ should include all scattering of the smectic layers whose traces are distributed in the [oa′b′c′o] plane (see figure 1 (*c*)). This means that the peak in the Φ-direction embraces the scattering of the smectic layers with tilt angles α distributed from Φ to α_{max}. An extreme case is the diffraction along the *Z*-direction, in which the smectic layers distribute from zero to α_{max} (see figure 1 (*b*)).

If we specify $I(\Phi)$ as the integral intensity of the small angle meridional reflection along the line with an angle Φ from the *Z*-direction (see figure 1 (*d*)), then the distribution function of the diffraction intensity P_Φ can be defined as

$$P_\Phi = \frac{I(\Phi)}{\int_0^\Phi I(\Phi)d\Phi}. \tag{10}$$

Suppose the correlation length is approximately the same in different angular directions around the normal to the smectic layers; then the distribution function of the scattering intensity $I(\Phi)$ is approximately proportional to the integration of the distribution function $P\alpha$ with an integration range from Φ to α_{max}. $P\alpha$ defines the probability of finding the smectic layers along the spherical lines lying with an angle α from *Z*-direction

$$\int_{\alpha=\Phi}^{\alpha_{max}} P_\alpha d\alpha = \frac{P_\Phi}{D_\Phi}, \tag{11}$$

D_Φ is a geometric factor indicating the ratio between the angle $\angle$b′oc′ and the angle $\alpha_{max} - \Phi$. For a given angle Φ, D_Φ can be derived from figure 1 (*c*) as

$$D_\Phi = \frac{\angle b'oc'}{\alpha_{max} - \Phi} = \frac{\arccos[\cos(\alpha_{max})/\cos(\Phi)]}{\alpha_{max} - \Phi}. \tag{12}$$

Finally, we can calculate the angular distribution of the smectic units from the two-dimensional diffraction patterns. It should be pointed out here that this is only valid for the smectic A phase with a continuous angular distribution in a relatively narrow angular range. In a future paper, we will discuss the different forms of the angular distribution of the smectic units, for example, in the form of a Gaussian function, and the influence on the small angle inner reflections [12].

3. Experimental

Two compounds have been investigated in this work. Their synthesis has been given elsewhere [5]. The molecular structures and mesomorphic transitions are given below:

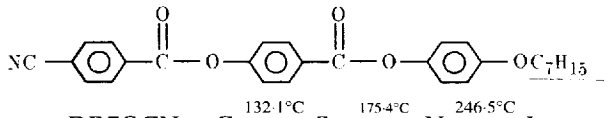

DB7OCN: C $\xrightarrow{132.1°C}$ S_A $\xrightarrow{175.4°C}$ N $\xrightarrow{246.5°C}$ I

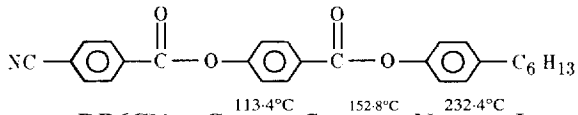

DB6CN: C $\xrightarrow{113.4°C}$ S_A $\xrightarrow{152.8°C}$ N $\xrightarrow{232.4°C}$ I

The liquid crystalline phases were characterized by differential scanning calorimetry (Du Pont 990) and polarizing microscopy (Leitz Orthoplan Pol, equipped with a Mettler FP52 hot stage).

For the X-ray measurements, the samples were put into a sandwich cell of thickness 1 mm. The sample holder was placed between two permanent magnets and fixed on a rotating stage (PO37). The permanent magnets produce a magnetic field of about 0·8 Tesla which aligned the samples. The rotating stage with the sample holder is part of an oven. The oven temperature was controlled by a regulator (Thor-PID) with an accuracy of ± 0·01 K. The oven is mounted in a focusing horizontal two-circle X-ray diffractometer (STOE STADI 2). The X-ray source is a long fine focus X-ray tube, Siemens FK, with a line focus

d-values of the small angle inner reflections for DB7OCN and DB6CN.

	DB70CN								
	Smectic A					Nematic			
T°C	132·2	141·7	150·9	161·4	171·8	176·9	186·4	199·5	234·9
d_1/Å	56·29	56·22	55·96	55·36	54·28	50·0	48·2	47·5	46·5
d_2/Å	28·16	28·04	27·94	27·72	27·21	27·2	27·1	—	—
d_1/d_2	1·999	2·005	2·003	1·997	1·995				
	DB6CN								
	Smectic A					Nematic			
T°C	115·6	125·4	134·9	143·6	149·1	153·1	177·3	195·0	222·9
d_1/Å	52·79	52·69	52·30	51·90	51·45	49·3	46·6	46·2	45·0
d_2/Å	26·46	26·33	26·20	26·03	25·79	25·7	25·6	—	—
d_1/d_2	1·998	2·001	1·996	1·994	1·995				

of 0·4 × 12 mm^2. The CuK_{α_1} radiation (λ = 1·54056 Å) is focused by a curved Ge(111)-monochromator. The mechanically and electrically controlled smallest stepwidth of the diffractometer was 0·001° in 2θ and ω. For fast diffractometry, a linear position sensitive detector (STOE Mini PSD) was used with a resolution of the stepwidth of 0·01° in 2θ. The X-ray diffraction was carried out using transmission geometry. A detailed description of the experimental set-up has been reported in [13].

Before starting the X-ray diffraction measurements, the samples were first heated to 3 or 4 K above the clearing point and then slowly cooled to the desired temperature. The entire measurements were performed in a cooling mode from higher to low temperature. The range of the scattering angles measured covered the interval $1° \leq 2\theta \leq 7°$ (for inner reflections) and $10° \leq 2\theta' \leq 30°$ (for outer reflections). Sufficient counts ($\geq 10^4$) were accumulated at the angle $2\theta_0$ to ensure the correct statistics of the scattering profiles. The fit of the peak profiles, with background correction and monochromator discrimination, was done using the STOE-package computer program [14]. The Lorentz and polarization corrections were made as described previously [2].

To check the alignment of the samples, X-ray flat photography was used before proceeding with the X-ray diffractometric measurements. Under this condition, the samples showed perfect orientation in magnetic field.

4. Results and discussions

As presented in the experimental part, both DB7OCN and DB6CN show the same phase behaviour but the phase transition temperatures for DB7OCN are clearly higher than those of DB6CN. The X-ray diffraction flat photography showed that the small angle meridian reflections in the nematic phase contain two diffuse spots for both samples. After the nematic–smectic A phase transition, the two diffuse spots are condensed into two intense quasi Bragg-like spots. The *d*-values of the [001] and [002] peaks are given in the table.

The table shows that the ratio d_1/d_2 is temperature independent in the smectic A phase. By comparison with the calculated molecular length, both compounds exist in a bimolecular modulation, the so-called A_2 phase [15]. After the smectic A_2-nematic phase transition, the smectic layer structure is destroyed and a rapid decrease in the *d*-values is observed. The nematic structure shows an incommensurable density fluctuation (see table 1). From the molecular formulae of DB6CN and DB7OCN, it is easy to understand that both samples are very favourably arranged in a head-to-tail fashion due to the longitudinal dipolar configuration in the molecules. The intensity ratio $I(002)/I(001)$ lies between 0·25 and 0·35. This is two to four times larger than that observed in normal smectic A phases [16]. This is evidence for a centrosymmetrical electron density distribution within the layers. The higher $I(002)/I(001)$ value can also be sometimes observed for an A_d phase with a partial bilayer structure [2].

The molecular configuration of DB6CN is simulated using an MNDO program [17], plotted in different perspectives, as shown in figure 5. The molecular length defined by the end-standing atoms, including their van der Waals' radii, amounts to 28·7 Å. It should be mentioned here that a dihedral angle of $\sim 70°$ is often observed between a neighbouring carbonyl group and a phenyl ring (–CO_2-phenyl ring) in the crystalline state [18], but the MNDO calculation gives a favourable molecular configuration in the gas phase and at zero temperature. The real dihedral angle in the liquid crystalline state may involve a distribution between 0° and 90°. By comparison with the thickness of the smectic layers in the table, it is evident that the smectic A_2 structure is stabilized through overlapping of the polar –CN end group.

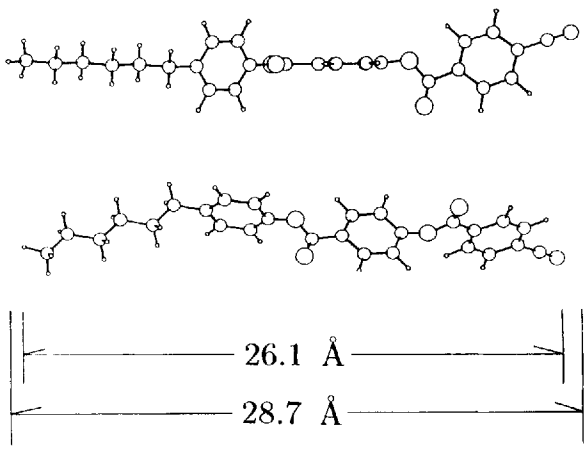

Figure 5. The molecular configuration of DB6CN, calculated by using an MNDO program, plotted for different directions.

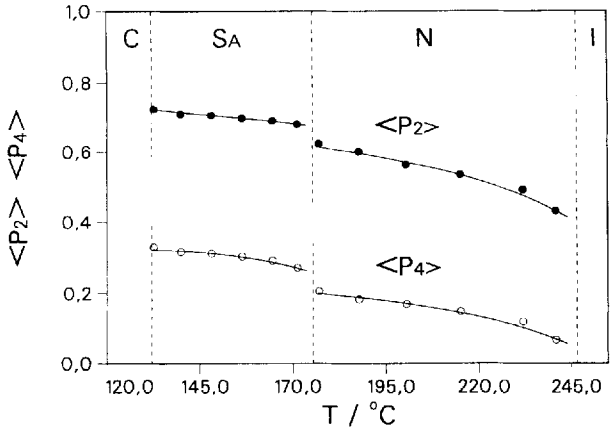

Figure 6. The orientational order parameter for DB7OCN.

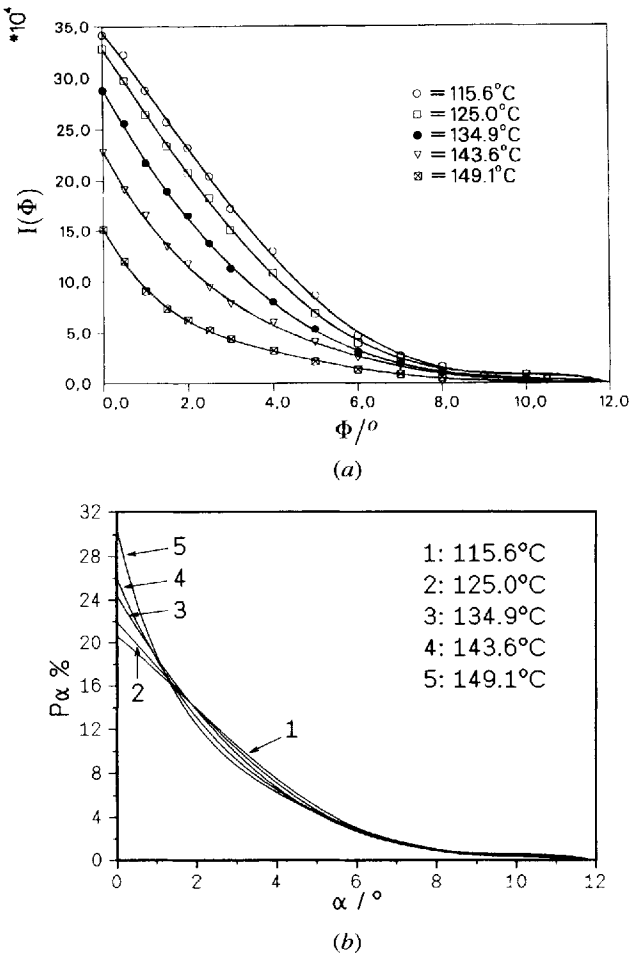

Figure 7. (*a*) The integral intensity $I(\Phi)$ at different temperatures for DB6CN. (*b*) The corresponding P_α profile versus the angle α.

The orientational order parameter for compound DB7OCN (see figure 6) is calculated using the method described in [2, 16]. Because the DSC measurements show a narrower peak at the smectic A_2–nematic phase transition, this is probably a first order phase transition [19]. The maximum value of $\langle P_2 \rangle$ amounts of 0·72 in the smectic A phase. Theoretically a first order smectic A–nematic phase transition may appear if the molecule shows a large ratio d_L/D (molecular length/molecular thickness) [20]. But for an exact assignment, measurements on a temperature scale smaller than 0·01 K during the phase transition are necessary.

In figure 7 (*a*), the temperature dependent integral intensity $I(\Phi)$ of the small angle inner reflection (001) is plotted versus the angle Φ for sample DB6CN. After normalization of the scattering intensity, one can find that the intensity distribution tends to concentrate on a small angle at high temperatures. A similar phenomenon is observed also by high resolution X-ray measurements [21]. An interpretation is that at lower temperatures the microdomains decompose into many small regions. In contrast, the smectic structure may melt to give larger domains at higher temperatures. However, it does not mean that the higher temperature structure is more regular or ordered. The small d_L values and the broad FWHM, as well as the lower $\langle P_2 \rangle$ at higher temperatures give evidence for the strong fluctuation of the smectic layers. This will result in reducing the correlation length. The corresponding P_α profile as a function of the angle α is given in figure 7 (*b*).

Using the method described in the theoretical part, the ratios ξ_{coh}/d_L are calculated from FWHM/$2\theta_0$ for the correlated smectic layers of DB6CN. Figure 8 shows that ξ_{coh}/d_L lies between 20 and 52 layers. The corresponding correlation length ranges from 1000 to 2700 Å. These values are in good agreement with the correlation lengths observed experimentally for a series of monomeric liquid

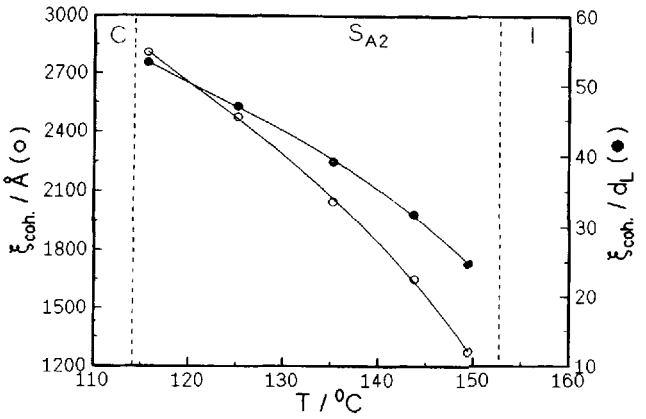

Figure 8. The correlation length itself and also the ratio of the correlation length to thickness of the correlated smectic layers ξ_{coh}/d_L as a function of temperature for DB6CN.

crystal materials (see table 1 in [22]). Under similar experimental conditions, i.e. the same thickness of sample and the same measuring time, the intensity of the small angle inner reflection for DB6CN is approximately 10 times stronger than that observed for 3,5-bis-(*p*-5-hexenyl-1-oxyphenyl)isoxazole [7]. This means that the smectic A_2 structure of DB6CN is comparatively more stable. The maximal distribution range Φ of the small inner reflection (see figure 1 (*d*)) is roughly up to 20° for 3,5-bis-(*p*-5-hexenyl-1-oxyphenyl)isoxazole and roughly up to 8° for DB6CN.

The smectic A_2 structure is also described as the so-called antiferroelectric array [15]. According to Prost [23], the smectic A_2 phase is especially stable and it costs a lot in elastic energy to demolish this structure. In most cases, the experimentally observed correlation lengths in smectic A_2 phases are clearly higher than those in monolayer smectic A phases [22, table 1].

5. Conclusions

In this paper, a method for determining the longitudinal correlation length of the smectic A phase is presented, which is based on our recently suggested diffraction model with undulation. After this model, the continuous angular distribution of the smectic layers has an influence on the structural stability and correlation length which cannot be ignored. The computer simulation was performed to reveal the relationship between the dimensionless parameters ξ_{coh}/d_L and FWHM/$2\theta_0$ for the diffraction profile in the form of the Lorentz function. Comparison of FWHM/$2\theta_0$, with the experimentally obtained diffraction data enables us to evaluate the correlation length directly.

This work was supported by the German Bundesministerium für Forschung und Technologie under Grant No. D.3-D05. We thank Dr Thomas Hanemann for useful discussions.

References

[1] FRANK, F. C., 1958, *Faraday Soc. Discuss.*, **25**, 19.
[2] FAN, Z. X., BUCHNER, S., HAASE, W., and ZACHMANN, H. G., 1990, *J. chem. Phys.*, **92**, 5099.
[3] FAN, Z. X., and HAASE, W., 1991, *J. chem. Phys.*, **95**, 6066.
[4] FEIGIN, L. A., and SVERGUN, D. I., 1987, *Structure Analysis by Small Angle X-ray and Neutron Scattering* (Plenum Press).
[5] CHIANG, L. Y., 1987, *Molec. Crystals liq. Crystals*, **146**, 137.
[6] STOE and CIE GmbH, 1993, *Powder Software* (*Software Manual*).
[7] FAN, Z. X., SEGUEL, C. G., AGUILERA, C., and HAASE, W., 1992, *Liq. Crystals*, **11**, 401.
[8] ALEXANDER, L. E., 1969, *X-ray Diffraction Methods in Polymer Science* (Wiley-Interscience).
[9] GREBYONKIN, M. F., PETROV, V. F., and OSTROSKY, B. I., 1990, *Liq. Crystals*, **7**, 367.
[10] ALS-NIELSEN, J., BIRGENEAU, R. J., KAPLAN, M., LITSTER, J. D., and SAFINYA, C. R., 1977, *Phys. Rev. Lett.*, **39**, 352.
[11] ALS-NIELSEN, J., LITSTER, J. D., BIRGENEAU, R. J., KAPLAN, M., SAFINYA, C. R., LINDEGAARD-ANDERSEN, A., and MATHIESEN, S., 1980, *Phys. Rev.* B, **22**, 312.
[12] FAN, Z. X., SCHUHMACHER, E., and HAASE, W. (in preparation).
[13] KLÄMKE, W., FAN, Z. X., HAASE, W., MÜLLER, H. J., and GALLARDO, H. O., 1989, *Ber. Bunsenges. phys. Chem.*, **93**, 478.
[14] STOE and CIE GmbH, 1987, *STADI Powder Software Manual* (unpublished).
[15] LEVELUT, A. M., TARENTO, R. J., HARDOUIN, F., ACHARD, M. F., and SIQAUD, G., 1981, *Phys. Rev.*, A, **24**, 2180.
[16] HAASE, W., FAN, Z. X., and MÜLLER, H. J., 1988, *J. chem. Phys.*, **89**, 3317.
[17] INDIANA UNIVERSITY, DEPARTMENT CHEMISTRY., 1997, *Quantum Chemistry Program Exchange, No. 523, MNDO version 4.01.*
[18] GEHRING, S., FAN, Z. X., HAASE, W., MÜLLER, H., and GALLARDO, H., 1989, *Molec. Crystals liq. Crystals*, **168**, 125.
[19] BAXTER, R. A., 1969, *Thermal Analysis*, Vol. 1, edited by R. F. Schwenker and P. D. Garn (Academic Press).
[20] MCMILLAN, W. L., 1971, *Phys. Rev.* A, **4**, 1238.
[21] DAVIDOV, D. (private communication).
[22] KELLER, E. N., HALFON, R., NACHALIEL, E., DAVIDOV, D., and ZIMMERMANN, H., 1988, *Phys. Rev. Lett.*, **61**, 1206.
[23] PROST, J., 1994, *Adv. Phys.*, **31**, 1.